HIGH-CURRENT ION LINEAR ACCELERATOR FOR MEDIUM-ENERGY PHYSICS (MESON FACTORY)

by

B. P. Murin, A. P. Fedotov, V. G. Kulman,
G. I. Batskikh and B. I. Polyakov

Radiotechnical Institute, USSR Academy of Sciences
Moscow, USSR

ABSTRACT

Main parameters and specific features of a 600-MeV linear accelerator, being designed to accelerate protons and negative hydrogen ions with an average current of 0.5 or 1 mA, are reviewed.

I. PECULIARITIES OF THE ACCELERATOR COMPLEX

The Meson Factory is being designed as a multipurpose instrument for implementing a wide range program of basic research in the nuclear and elementary particle physics. Moreover, the high intensity of proton and secondary beams opens up prospects for various applications such as neutron generation, biomedical research, radiation physics, nuclear chemistry, and large scale production of the radioisotopes not obtainable in a nuclear reactor.[1,2]

The Meson Factory is essentially a 600-MeV proton linac with 0.5 mA average beam current, 1% duty factor and 100-μsec pulse length. In the future, the average beam current is to be brought up to 1 mA. It is planned to accelerate both proton and negative hydrogen ions simultaneously (with an average current of 50 μA at the first stage of the project).

In choosing the accelerator complex layout, the aim was to meet the experimental physics requirements while saving costs whenever it was possible.

As the construction cost of a proton linac is proportional to the square root of the duty factor, the former was chosen rather small (1%). A storage ring with negative hydrogen ion charge exchange injection at the linac output offers the best opportunities for the experimental physics. Slow proton extraction from the storage ring makes it possible to have a continuous proton current (an average value of about 20 μA at the first stage of the project), which is of special importance for the meson physics program.

When used as an injector, either for a superconducting proton linac or for a proton synchrotron, this complex is easily convertible into a high-current kaon factory.

The main peculiarity of the accelerator complex is a combination of a linac to accelerate protons (as well as negative hydrogen ions) at a rather small duty factor and a storage ring using negative hydrogen ion charge exchange injection and slow beam extraction.[1]

Distinguishable features of the 600-MeV, 0.5-1 mA proton linac itself are:

1. An odd harmonic ratio between the accelerating fields in the first and in the second stages of the linac permits acceleration of both protons and negative hydrogen ions simultaneously.

2. In the main (second) stage of the linac, a new type of $\pi/2$-mode accelerating structure is to be used. This will be either an annular side-coupled structure having a wider dispersion curve[3]

than that of LAMPF[4] or a disc-and-washer loaded one[5] with several times as wide dispersion curve as that of LAMPF.

3. A system that damps coherent oscillations is incorporated to avoid the beam loss at the transition between the first and the second stages.[6]

4. Stand-by rf power amplifiers are used to reduce significantly the accelerator MTBF.

5. An option of adding a beam extraction system at 160 MeV and an energy control system to vary the energy continuously between 160 and 600 MeV is envisaged.

II. LINAC BLOCK-DIAGRAM AND BASIC PARAMETERS

Figure 1 shows the block-diagram of the linear accelerator. The linac has two stages. The first one comprising 5 tanks (T_1 to T_5) with drift tubes and field stabilizing post couplers* accelerates protons and negative hydrogen ions up to 100 MeV. The operating frequency is 198.2 MHz. The length of this stage is about 70 meters.

Further acceleration is achieved in the second stage composed of 28 tanks† (T_6 - T_{33}) operating at 991 MHz. Each tank consists of four sections (S) intercoupled by bridge couplers (BC). The second stage is about 360 m long while the total length of the linac is about 450 m.

In the first stage each tank is fed from an amplifier channel (AC-I) containing a power amplifier (A) and a modulator (M). In the output stage of the amplifier a 4 MW peak power metal-ceramic triode is used. Each of the second stage tanks is driven by a 4 MW peak power klystron amplifier (AC-II). The power driver (PD) comprises master oscillator-amplifier (MO-A) and two drivers (DI and DII).

The beam is focused by magnetic quadrupoles (in the first stage) or by magnetic doublets (DM) (in the second stage). Beam matching with respect to the transverse motion at the transition between the two stages is effected by a matching device (MD) consisting of 4 quadrupole magnet lenses.

Two simultaneously operating 750-keV injectors, i.e., a proton one (PI) and a negative hydrogen one (NHII) are installed at the accelerator input. A third injector, i.e., that of polarized ions (PII) is planned to be installed later.

Computer control and monitoring of all linac systems are being contemplated.

Basic parameters of the linac are listed in Table I.

III. PARTICLE DYNAMICS

Acceleration of an average current as high as 0.5 or 1 mA raises an urgent problem of preventing particle loss. Therefore, special consideration was given to calculation of beam motion. From the results of this calculation, the linac parameters have been chosen and the rf and geometric tolerances have been determined to exclude any particle loss. Also, requirements on the automatic control systems to keep the tolerances within permitted limits have been found.

The effect of random disturbances was studied by the statistical tests method (the Monte Carlo Method).[7] Computer modeling of perturbed motion has shown the tolerances on rf field amplitude and phase (about 1% and 1°, respectively) to be insufficient to suppress bunch center-of-mass oscillations. The displacement of bunch c.m. at the output of the first linac stage can be as high as ±25° in phase (at a frequency of 991 MHz) and ±0.3% in momentum while the respective bunch dimensions are 90° and 0.8%. On the other hand, the bucket at the input of the second stage is 100° wide in phase and 1.35% wide in momentum. Thus, at the transition between the two stages it appears necessary a) to damp the longitudinal oscillations of bunch c.m., and b) to compress the bunch phase width (by stretching the beam momentum spread) in order to match it better with the second stage bucket. A system of damping the coherent oscillations[6,7] is expected to cope with the first problem. With the tolerances accepted, this system eliminates 50% of momentum spread increase and 80% of bunch phase-width increase.

The second task, i.e., that of bunch transformation is solved by increasing the frequency of longitudinal oscillations in the $\lambda/4$-tank 5 by a factor of 1.4 through shifting the synchronous phase up to 60°.[7]

*These couplers are absent in the short-length tank 5.

†One of these tanks placed at the 160 MeV beam extraction line is essentially a matching cavity.

The strong focusing channel also has some peculiarities. Measures have been envisaged to prevent beam radius growth in the first stage due to the idle gaps between the tanks. Each of these gaps, approximately $\beta\lambda/2$ long, can cause a beam radius increase by a factor of 1.5. In order to avoid this growth, the magnet lenses in the end half-tubes of each gap have opposite polarities and magnetic gradient therein is increased by about 30%. Computer modeling has shown this structure of transition section to be capable of eliminating essentially all of the beam growth caused by the effect of intercavity gaps the lengths of which are less than $\beta\lambda$.

The main reasons for the beam radius being perturbed proved to be the gradient errors and the lens median plane position errors that either do not vary or vary very slowly during accelerator operation. The corresponding beam changes in the first stage will be compensated for by correcting the gradients in the last four lenses of this stage. A possibility of such compensation has been verified by computer modeling. Figure 2 shows the beam radius as a function of the consecutive number of accelerating period when the correction either is or is not made.

A beam position control system is being designed to reduce the beam c.m. transverse oscillations along the accelerator.

Thus, in devloping the linac, much attention is given to methods and systems of correcting for slow perturbation of beam parameters.

Figure 3 shows the beam radius and the beam c.m. displacement as a function of the consecutive number of focusing period in the second stage. Tables II and III cite characteristics of longitudinal and transverse motion of particles in the linac.

Smooth energy variation between 160 and 600 MeV is introduced into the second stage design. This energy range is covered stepwise by switching off the required relevant number of tanks while within each step the energy is smoothly adjusted by varying the rf amplitude or phase in the last of the acting tanks to drive it into a nonresonant acceleration mode. The entire energy range is covered easily due to the fact that the tanks in the second stage are rather short and the longitudinal oscillation phase change per tank is small.

Investigation of beam spectrum with the energy controlled by rf phase variation alone has shown that the spectrum width increases by not more than 20% if the energy is varied from 450 to 600 MeV. Figure 4 shows the dependence of beam energy (W) and beam velocity spread $\beta\beta_s/\beta$ at the output of tank 25 upon rf field phase $\Delta\phi$, with the field amplitude kept constant. Dotted lines show the input and the output energy in this tank (W_{in} and W_{out}). Transverse oscillation phase change across this tank is 0.18. That is why the full energy range coverage in tanks 20 to 33 can be easily obtained by means of rf phase variations alone (from 0 to 120°). However, in tanks 10 to 19 both phase and amplitude variation are required to control the energy.

IV. ACCELERATING SYSTEM

The accelerating system of the first stage consists of 5 tanks with drift tubes and post couplers.

Two $\pi/2$-mode structures have been designed at this Institute for an energy between 100 and 600 MeV. One is an annular side-coupled structure. Its calculated effective shunt impedance is between 33 and 52 MΩ/m in an energy range from 100 to 600 MeV. The experimental values are 20 or 25% lower due to rf power losses in the couplers and due to a difference between actual and theoretical surface resistance of copper. Dispersion curve width is about 10%. With this width the frequency separation between undesirable modes is large enough to provide the necessary field stabilities with the fabrication tolerances (of a class 2 or 3 standard) met rather easily.

The procedure to be used in fabricating the structure is being perfected, and a possibility of forming cells by stamping is being studied. Few cells have already been obtained by stamping. The cell design enables one to braze a multicell tank in a hydrogen furnace during one heating cycle. Figure 5 shows a full scale model of the tank. The end faces are provided with metal vacuum gaskets.

The second structure, i.e. that with washers and discs, is shown in Fig. 6.[5] It is a cylindric cavity alternately loaded with conducting washers (1) and discs (2). The washers are supported by metal stems (3) placed in the rf electric field mode. This structure is essentially a chain of coupled cells of 2 types, i.e. an accelerating one formed by the space between washers near the axis and a coupling one formed by the space between discs near the outer wall. Each two adjacent cells

are coupled through a circular slot between the washer and the disc. Since the coupling is strong the dispersion curve width is about 50%, this makes the frequency separation between undesirable modes and the field stability in this structure more favourable than in other ones. Figure 7 shows the dispersion curve of a disc-and-washer loaded structure. The operating point is in the center of the dispersion curve. The calculated effective shunt impedance is 25 to 50 MΩ/m in an energy range from 100 to 600 MeV.

Each tank has 4 sections intercoupled through resonant bridges, the rf power being fed into the middle one.

V. RF POWER SUPPLY AND FIELD STABILIZATION SYSTEMS

A characteristic feature of triode and klystron amplifiers used in the first and in the second stages of the accelerator is a high peak and average output rf power. This is illustrated in Table IV.

Two high-power experimental facilities that model two typical linac stages are being constructed at this Institute to elaborate the design of power amplifier channels, tanks, sections, and control systems.

Figure 8 shows the first model of a power amplifier (in the mounting stage) using a grounded-grid triode. The anode tank is designed to be filled with dry compressed (up to 2.5 atm) nitrogen to provide for a sufficient resource of electric strength. The anode modulator uses a partial discharge of a capacitor battery through a switching tube.

The pulse modulator for the klystron amplifier of the second stage uses a full discharge of a capacitor battery. Linear charging of battery results in uniform power consumption from the mains. Switching by high-power silicon diodes and thyristors provides for a better reliability of modulators. The power is supplied from a stabilized thyristor rectifier. An efficient fast acting system protects the klystron amplifier in case of a breakdown.

The redundancy of rf power supply provided by one standby rf power channel in the first stage and by three in the second stage will result in more dependable operation. A standby channel is coupled to the tank through a coaxial switch or through a waveguide switch in the first and the second stage, respectively, to replace the failed channel. Calculations show this redundancy reduces the mean time between failures by a factor of 4.5 times.

In order to meet the required tolerances on the field stability in a tank severely loaded by beam, the automatic control system has been conceived as a combination of a programmed system using a primary signal and of a negative feedback system. The former eliminates basic perturbations due to beam loading while the latter eliminates all other perturbations including the instability of rf amplifier channel. The beam envelope is used as a primary control signal for the former system.

Figure 9 shows a simplified block-diagram of rf field control system. The rf amplitude and/or phase are stabilized by actuators, i.e. by a controlled amplifier stage (CA) with a fast ferroelectric phase shifter* to control the amplitude and/or phase in the first stage and by a travelling wave tube (TWT) that combines both phase and amplitude control of driving rf power in the relevant channel of the second stage.

Calculations made for the control systems of the first stage show that the static stabilization factor of a negative feedback system can be as high as 40-50, and the cut-off frequency is about 300 kHz.

In the second stage, the static stabilization factor of phase amplitude control systems is only a few units due to small buildup time of the tank and due to larger time delay in the control loop (additional delay in the klystron). More efficient operation of the control systems is provided by a "forerunner," i.e., a device inserted into the feedback loop to compensate the feedback loop delay, which results in a 10 times increase of static stabilization factor without impairing the control system bandwidth.

At the transition between the two linac stages a coherent phase oscillation damping system is provided which will use a beam-referred phase control system (PC-B) (Fig. 9).[6]

All tanks are tuned by stabilizing the temperature of tank material. To this end, either the cooling water temperature or the water flow is varied.

---

*The fast phase shifter is a part of a phase shifting unit that includes also the actuator of a slow phase control system.

The accuracy of maintaining the tank eigenmode frequency in terms of phase is ±15 degrees.

REFERENCES

1. B. P. Murin, Proc. of the 8th Intern. Conf. on High Energy Accel., CERN, 1971, p. 540-547.
2. L. Rosen, Physics Today, 20, 21 (1966).
3. V. G. Kulman, E. A. Mirochnick, V. M. Pirozhenko, Prib. Tekh. Eksp., No. 4, 56 (1970). In Russian.
4. E. A. Knapp, B. S. Knapp, J. M. Potter, Rev. Sci. Instr. 39, 979 (1968).
5. V. G. Andreev, V. M. Pirozhenko, Trudy Radioteknicheskogo Instituta Akademii nauk SSSR (Proc. of the Radiotechnical Inst., USSR Academy of Sciences) No. 9 (1971). In Russian.
6. B. P. Murin, "Stabilizatsiya i regulirovanie vysokochastotnykh polei v lineinykh uskoritelyakh ionov" (RF Field Stabilization and Control in Ion Linear Accelerators) Atomizdat, Moscow (1971). In Russian.
7. B. P. Murin, B. I. Bondarev, L. Yu. Solovyev, IEEE Trans. Nuc. Sci., NS-18, 621 (1971).

TABLE I

BASIC PARAMETERS OF 600-MeV, 0.5-mA LINAC

Parameter	First Stage	Second Stage
Injection energy, MeV	0.75	100
Output energy, MeV	100	600
Accelerating field frequency, MHz	198.2	991
Proton beam pulse length, μsec	100	100
Pulse repetition, pps	100	100
Duty Factor, %	1	1
Peak beam current, mA	50	50
Output momentum spread, %	±0.6	±0.4 No debuncher
		±0.1 With debuncher
Normalized effective input emittance, cm·mrad	0.23π	1.24π
Normalized effective output emittance, cm·rad	1.24π	4.4π
Number of tanks	5	28
Tank diameter, cm	108,86, 86,86,86	40
Tank length, m	16.8,16.1, I5.6,13.2,6.4	8 to 13
Peak rf power into beam, MW	5	25
Peak rf power loss in walls, MW	8.0	53
Total peak input rf power, MW	13	78
Total average input rf power, MW	0.65	0.9

TABLE II

CHARACTERISTICS OF LONGITUDINAL MOTION

	Parameter	Stage I	Stage II
Accelerating channel parameters	Synchronous phase in corresponding tanks, degrees	32 to 37 26,26,26 60	33
	Bucket width in momentum, %	10	1.35
	Period minor longitudinal oscillations, m	0.9-24	16-78
Accelerating channel rms errors	Tank length error,m	1.10^{-3}	
	Drift tube len th, error, %	7.10^{-2}	
	Drift tube positioning error, %	3.10^{-5}	
	Relative positioning error, %	2.10^{-4}	
	Fabrication error per accelerating cell, m		10^{-4}
	Intertank gap error,m		10^{-4}
	Avg. rf field amplitude instability, %	1	1
	Field nonuniformity,%	1	5
	Rf amplitude difference between tank sections, %		0.5
	Rf phase difference jitter between tanks, °	1	1
Beam parameters (max. values)	Bunch phase width (f=200 MHz), °	100 to 19.5	19.5 to 13
	Momentum spread, %	10-1.2	1.2-0.8
	Beam c.m. displacement at the output: a) in phase (f=200 MHz),°	0-±7.5	±1-±4.5
	and b) in momentum, %	0-±0.5	±0.1 to ±0.22

TABLE III

CHARACTERISTICS OF TRANSVERSE MOTION

Parameter	Stage I	Stage II
Focusing Channel Parameters:		
Defocusing parameter (A)	0.4 - 0.07	0.5 - 0.07
Quadrupole lens parameter (Λ^2)	7.2 - 8.8	42 - 55
Focusing period length, cm	$2\beta\lambda$	222 - 349
Drift tube length to focusing period length ratio	0.375 - 0.25	
Tank length, cm		122 - 261
Lens centers separation in a doublet, cm		26.5
Pole length, cm		18.5
Magnetic field gradient,* kGs/cm	5.89 - 0.78	2 - 2.5
Aperture diameter, cm	1.5 - 3.0	3.4 - 3.8
Number of quadrupole (or doublet) lenses	186 +10 half-tubes	113
Relative radial oscillation frequency ν (minimum value per period length)	0.43 - 0.6	0.6
Normalized acceptance, cm·mrad	$(0.8 - 5.0)\pi$	$(3.8 - 6.9)\pi$
Focusing Channel rms Errors:		
Magnetic field gradient instability in a quadrupole lens, %	0.2	0.1
Quadrupole lens azimuthal, degrees	0.5	0.3
Magnetic lens axis displacement from geometrical axis, mm	0.05	0.05
Drift tube target sighting error, degrees	2.10^{-4}	2.10^{-4}
Accelerating section target sighting error, degrees	6.10^{-4}	6.10^{-4}
Target positioning error, mm	0.02	0.02
Beam parameters:		
Beam current, mA	50	50
Injector output phase-space density, A/cm mrad	1	
Beam diameter, mm	8 - 15	20 - 28
Beam axis displacement,† mm	0 - 5.5	1 - 8.5
Effective normalized emittance, cm mrad	$(0.23 - 1.24)\pi$	$(1.24 - 4.4)\pi$

* Calculated per drift tube length
† With correction

TABLE IV

PARAMETERS OF RF AMPLIFIERS

Parameter	Stage I Triode Amplifier	Stage II Klystron Amplifier
Peak power, MW	4	4.75
Average power, kW	150	60
Pulse Length, μsec	300	115
Modulator peak power, MW	11	15
Modulator output voltage, kV	40	80

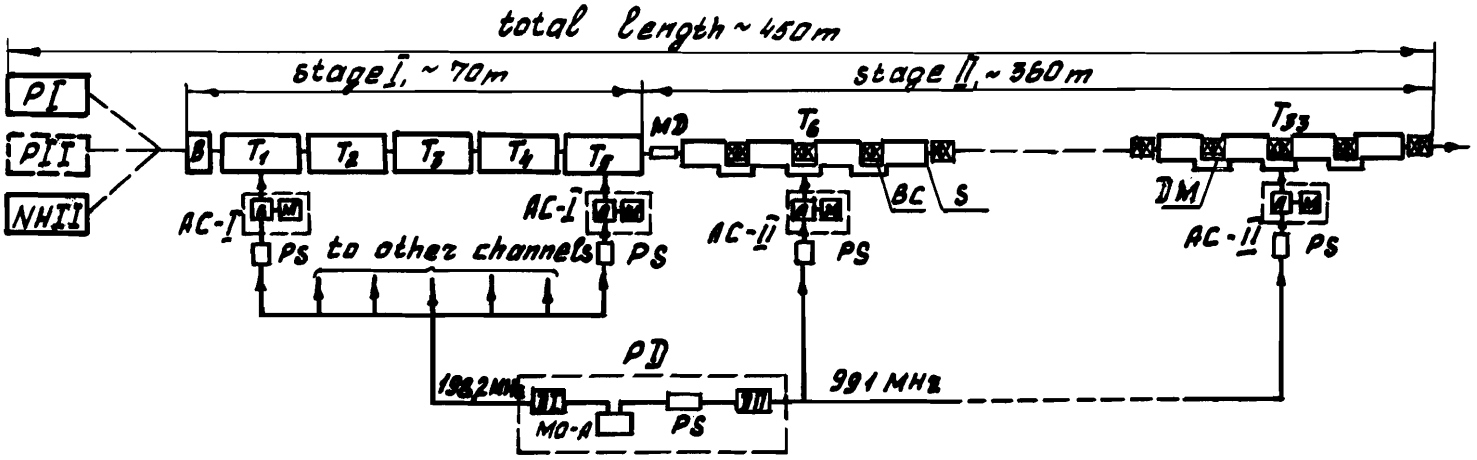

Fig. 1 Block diagram of 600-MeV proton linear accelerator where: PI, proton injector; PII, polarized ion injector; NHII, negative hydrogen ion injector; B, buncher; T_{1-33}, tank; MD, matching device; AC, amplifier channel; BC, bridge coupler; S, section; DM, magnet doublet; A, RF amplifier; M, modulator; PS, phase shifting unit; PD, power driver; D, driver; MO-A, master oscillator-amplifier.

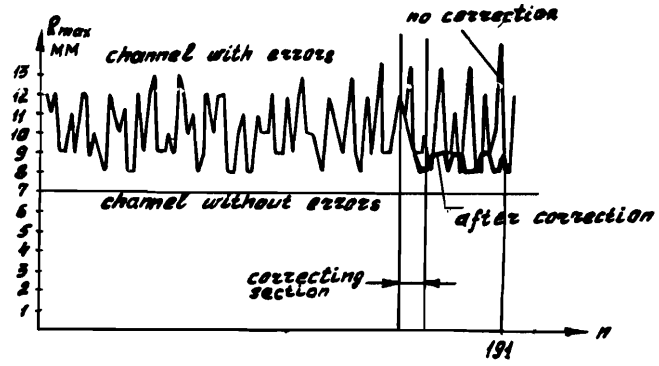

Fig. 2 Correction of beam transverse dimension.

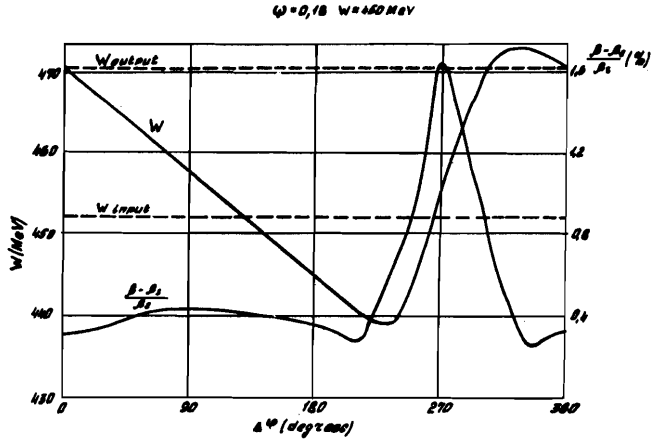

Fig. 4 Energy and velocity spread vs field phase.

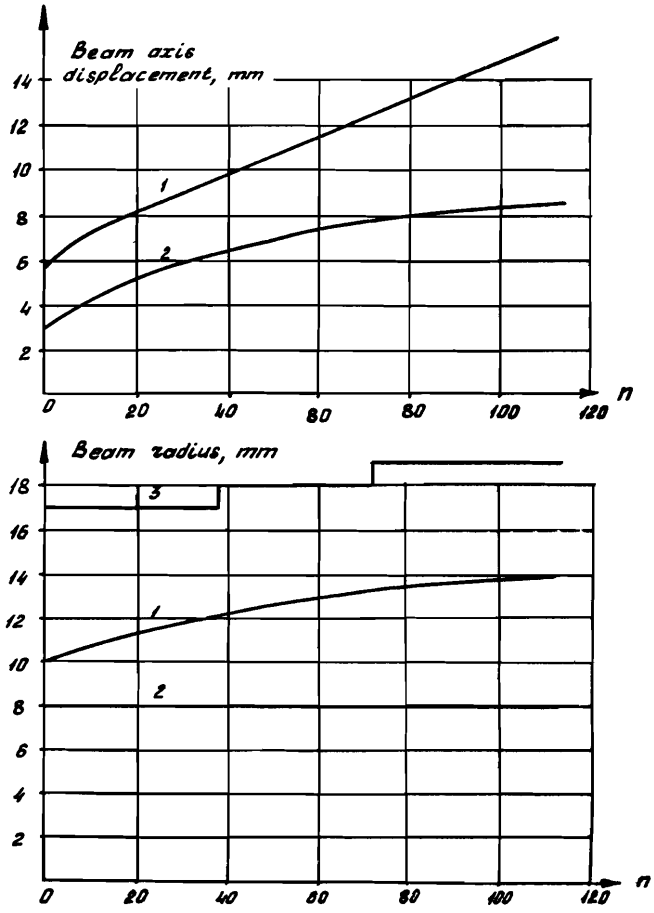

Fig. 3 The beam radius and the beam c.m. displacement as a function of consecutive number of focusing period.

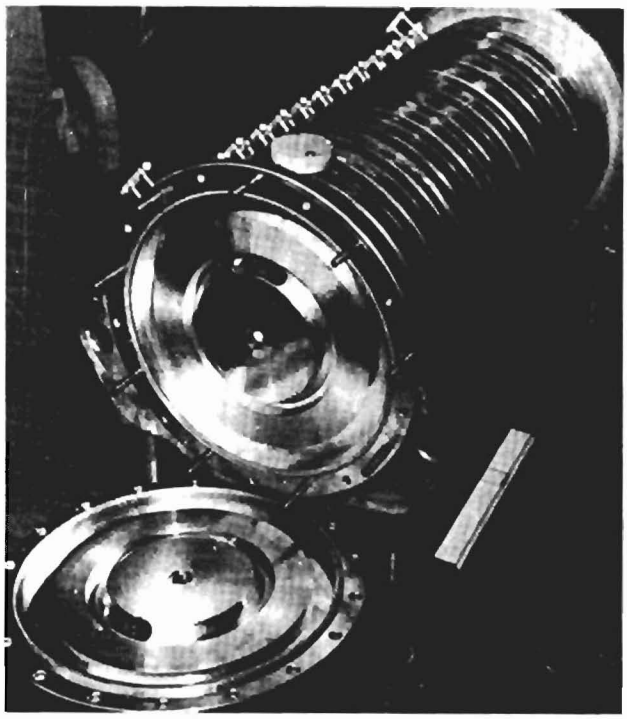

Fig. 5 Full scale model of a tank

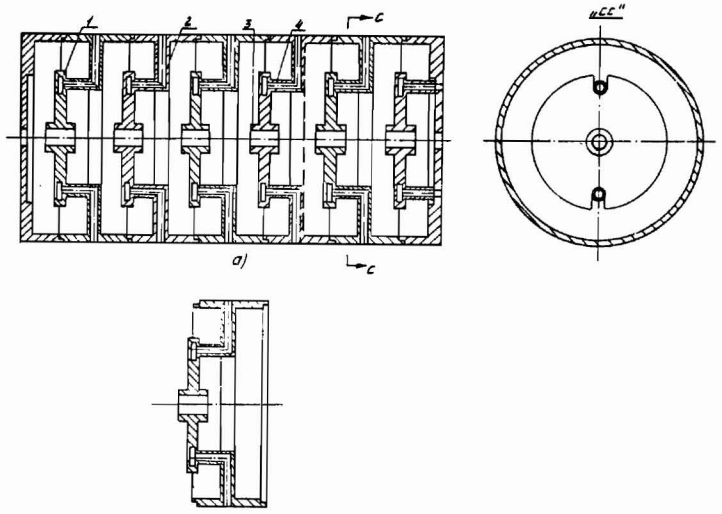

Fig. 6 Accelerating structure loaded with washers and discs

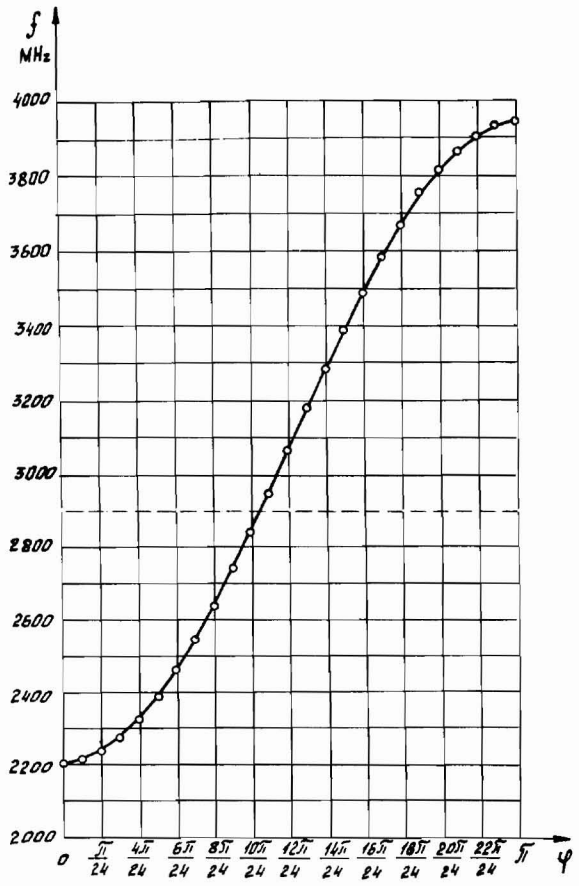

Fig. 7 Dispersion curve of a disc-and-washer loaded structure.

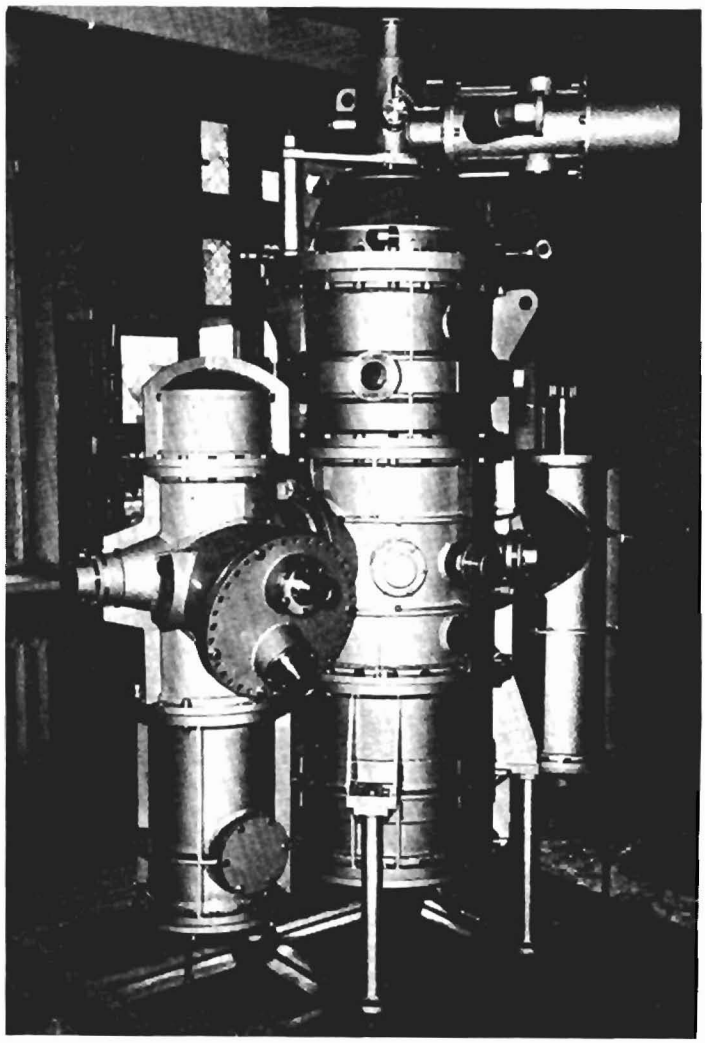

Fig. 8 First model of a power amplifier (in the mounting stage) using a grounded-grid triode.

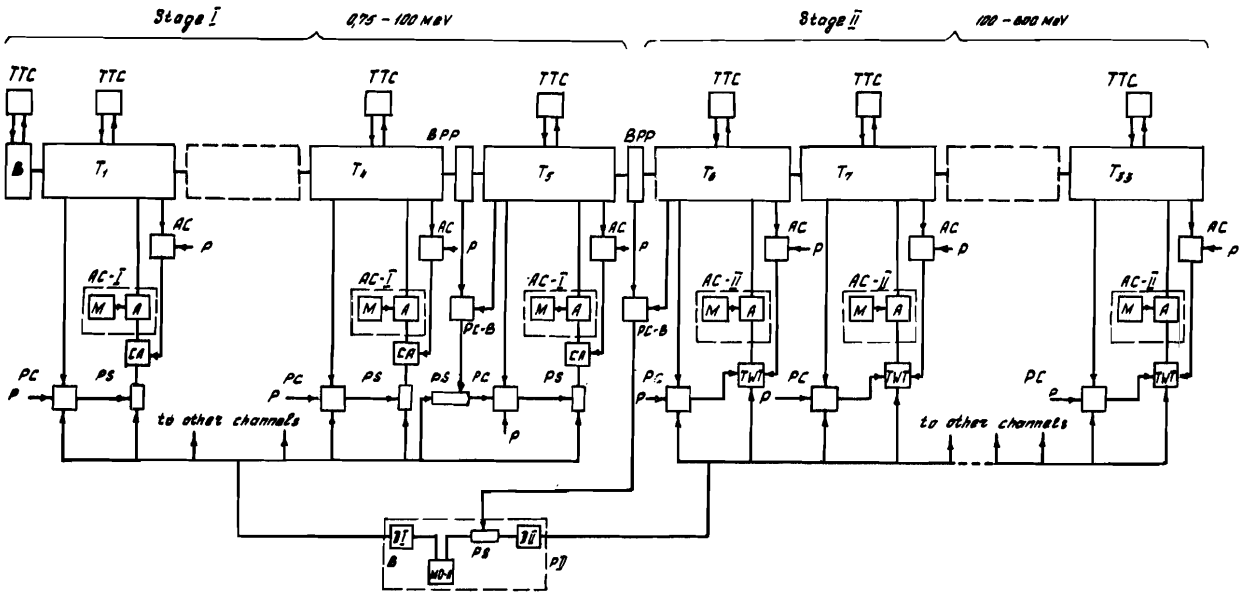

Fig. 9 Simplified block diagram of rf field control system where: B, buncher, T_{1-33}, tank; M, modulator; A, rf amplifier; AC-I and AC-II, amplifier channels; CA, controlled amplifier; AC, amplitude control; PC, phase control, PC-B, beam referred phase control; TTC, tank tuning control; TWT, traveling wave tube; P, programmed pulse; BPP, beam phase probe; PD, power driver; D, driver; MO-A, master oscillator-amplifier; PS, phase shifting unit.